Mask Defect Auto Disposition based on Aerial Image in Mask Production

C.Y. Chen[a], Laurent Tuo[a], C. S. Yoo[a], Linyong Pang[b], Danping Peng[b], Jin Sun[b]
[a]E-Beam Operation Division, Taiwan Semiconductor Manufacturing Company (TSMC), 25 Li-Hsin Rd. Hsinchu, Taiwan 300-77, ROC
[b]Luminescent Technologies, Inc., 2471 East Bayshore Road, Suite 600, Palo Alto, CA 94303, USA

ABSTRACT

At the most advanced technology nodes, such as 45nm and below, aggressive OPC and Sub-Resolution Assist Features (SRAFs) are required. However, their use results in significantly increased mask complexity, making mask defect disposition more challenging than ever. In an attempt to mitigate such difficulties, new mask inspection technologies that rely on hardware emulation and software simulation to obtain aerial image at the wafer plane have been developed; however, automatic mask disposition based on aerial image is still problematic because aerial image does not give the final resist CD or contour, which are commonly used in lithography verification on post OPC masks. In this paper, an automated mask defect disposition system that remedies these shortcomings is described. The system, currently in use for mask production, works in both die-to-die and die-to-database modes, and can operate on aerial images from both AIMS™ and aerial-image-based inline mask inspection tools. The disposition criteria are primarily based on wafer-plane CD variance. The system also connects to a post-OPC lithography verification tool that can provide gauges and CD specs, which are then used in the mask defect disposition.

.

Keywords: Mask inspection, mask defect review, mask defect disposition, aerial image, AIMS

1. INTRODUCTION

As semiconductor manufacturing processes advance in step with Moore's Law, the photomask industry has been increasingly challenged, especially as it entered the sub-wavelength era. When imaging at subwavelength, resolution enhancement technologies (RET) such as OPC, Phase Shift Masks (PSM), and sub-resolution assist features (SRAFs), are often required, adding complexity to the mask[1-7]. For example, at subwavelength, mask patterns diverge from target design and wafer image, phase defects seen on inspection images differ from wafer images due to the different wavelengths used in mask inspection system and wafer scanners, and because of optical proximity effects the severity of mask defects no longer correlates with their size on the mask. To meet these challenges, mask inspection, review, and disposition increasingly rely on aerial image analysis. An aerial image is equivalent to the intensity image from a scanner; it is related to the wafer print CD, but does not provide the wafer CD directly. The Aerial Image Measurement System (AIMS), which captures mask aerial images at the same wavelength as the scanner illuminator, has become an essential tool for both pre- and post-repair mask defect review. For inline mask inspection, aerial images are added either through hardware or simulations.

Figure 1 depicts a standard mask inspection and repair flow. First, a mask is inspected with an inline inspection system. The detected defects are then reviewed by operators to classify and separate nuisance defects from real defects. However, some defects are marginal, and therefore require aerial image review using AIMS. Once the AIMS review is performed, the remaining real defects requiring repair are identified, and the mask is sent to the repair system. After mask defect repair, one more round of AIMS review is performed to ensure the repair is successful and the mask can meet the spec. This step is necessary because the repair process may introduce transmission or phase defects.

An aerial-image-based mask inspection system can provide a cost-effective alternative to traditional inline mask inspection. Such an inline inspection system is currently under evaluation at TSMC EBO. In this case, an offline mask defect disposition based on the aerial images from such inspection system is also required.

As the internal mask shop of the world's leading foundry, TSMC EBO processes more than 5000 masks per month, or more than 167 masks per day. On average, there are tens to hundreds of defects per mask requiring AIMS review and disposition. A useful aerial-image-based automatic mask defect disposition system would need to be able to handle this throughput by performing a fast, accurate and consistent mask defect disposition consistent with the litho verification spec used in OPC. The challenges of developing this system are discussed and addressed in this paper.

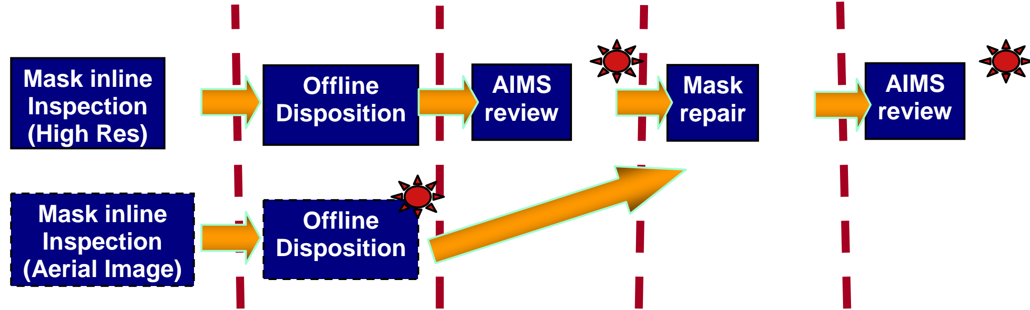

Fig. 1. A standard mask inspection, review, repair and disposition flow. The "*" symbol highlights where a mask defect disposition based on aerial image is required.

2. METHDOLOGIES

2.1 Manual Flow to Disposition Mask Defects Based on Aerial Images

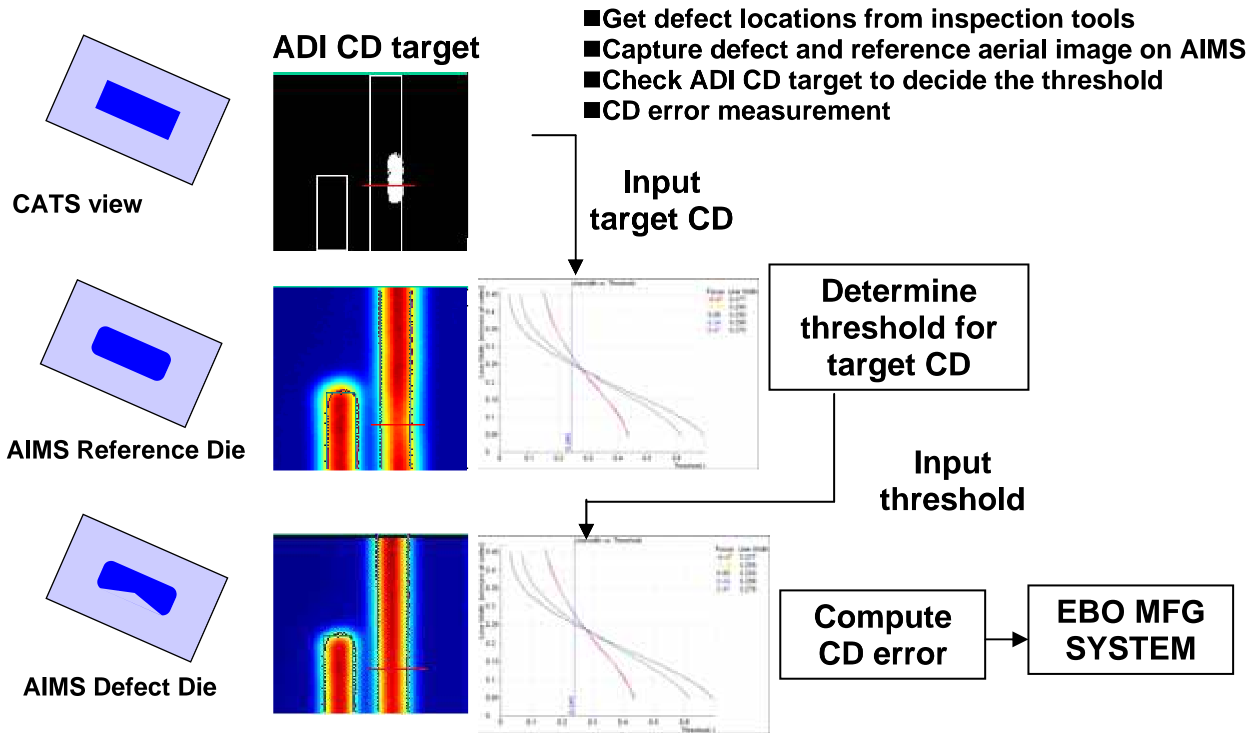

Fig. 2. Manual flow to disposition mask defects based on aerial images

Figure 2 shows the manual flow performed by operators. First, the defect location is obtained from the inspection system. Second, the coordinates are passed to AIMS, the stage is moved to the corresponding location on the mask, and the defect aerial image is taken. The reference image is also taken from the same location on another die by AIMS. Third, using the AIMS software, one can determine the threshold to print the target CD on the reference aerial image.

Fourth, using the same software, a defect CD can be calculated by applying the same threshold to the defect aerial image. In the final step, the CD error is calculated and reported to TSMC EBO's MFG system.

This complicated procedure must be repeated for each defect because a single threshold is not accurate enough to be applied to all features on the mask (similar to applying a variable threshold model in OPC). Because this procedure is so complicated and tedious, and considering TSMC's EMO output of more than 5000 masks per month, it is easy to see that the opportunity for operator error during this manual disposition is significant. In the new flow enabled by Luminescent's Automated Image Processor Hub (LAIPH, pronounced "life"), the disposition of mask defects is fully automated.

2.2 The Challenges for Mask Defect Disposition based on Aerial Image

The many challenges of fully automatic aerial-image-based mask disposition are best identified and explained through an example.

The first problem which must be addressed is that the two aerial images from AIMS are not perfectly aligned because the AIMS stage is not accurate enough (Figure 3). In order to identify the defect location and determine the wafer target CD, the defect and reference images must be aligned.

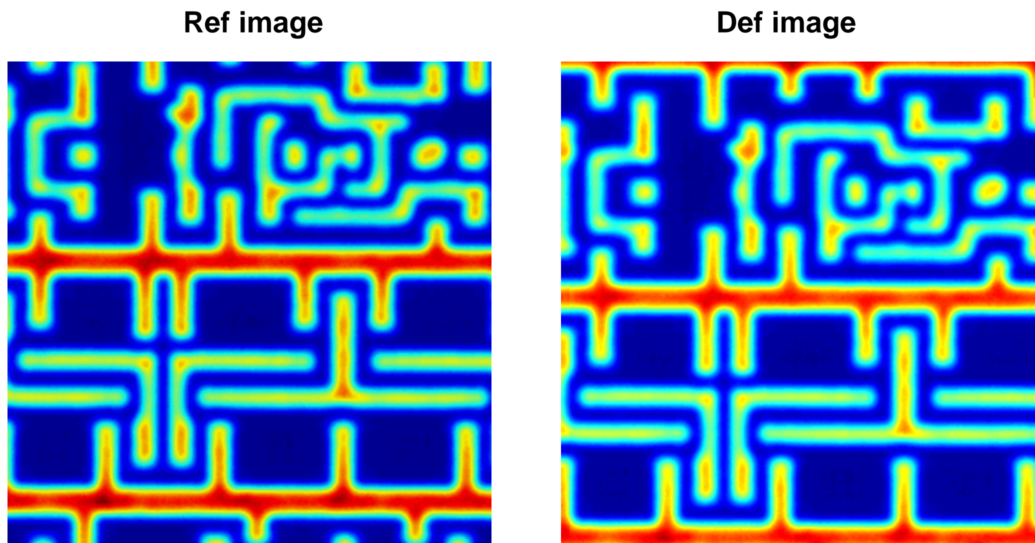

Fig. 3. Problem to solve: 1. The two aerial images (reference and defect) are not perfectly aligned.

The second problem which must be overcome is that the design GDS database is needed to obtain the wafer target CD, but since the defect image coordinates obtained from mask inspection is neither in design coordinates nor very accurate, the corresponding design clip must be located and obtained from the large GDS file. But, how? To make matters worse, the alignment has to be performed between an aerial image and design GDS - two very different image types. The aerial image is a smooth, gray-scale image, while the GDS design is composed of a number of polygons (Figure 4).

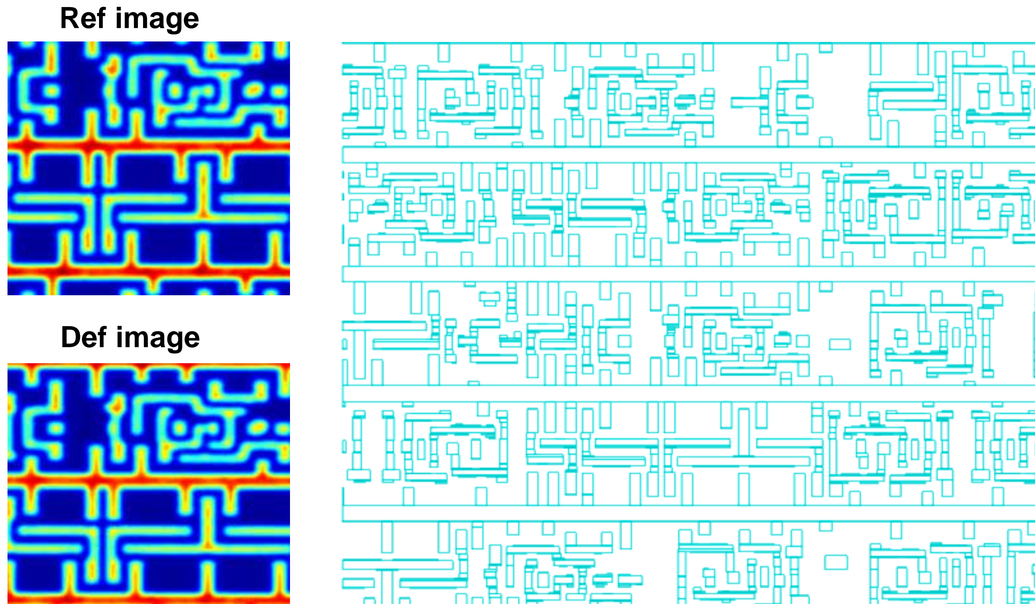

Fig. 4. Problem to solve: 2. How to find the corresponding design from the design database

The third problem is that once the wafer target CD and aerial image intensity for both defect and reference are ready, the wafer CD changes must be derived. The flow performed by the operator is as follows (Figure 5): After the reference image and defect image are aligned, and the defect location is identified, a cutline is drawn on the aerial image at the defect location. Based on the wafer target CD, the threshold is adjusted until it produces the target CD on the reference aerial image intensity. The same threshold is then applied to the defect aerial image intensity curve to determine the defect CD. In some cases, the CD changes at other doses must also be evaluated. In such case, the threshold must be changed and the CD re-measured.

Fig. 5. Problem to solve: 3. How to derive wafer CD changes from aerial images of defect and reference

2.3 Overview of the Mask Defect Auto Disposition Based on Aerial Image

In the aerial-image-based mask defect auto disposition system that is deployed at TSMC, the following features are available: all defects in the field of view can be automatically detected, not just a single defect; mask defects are dispositioned based on CD changes, using the same CD tolerance rules as TSMC's OPC litho verification system; CD changes are automatically calculated using the defect image, reference aerial image and the design target GDS; multiple cutline locations, multiple thresholds, and even defocus aerial images are supported; the GUIs are intuitive and easy-to-use, allowing operators and engineers to review the final results; all runs are distributed, so a very high throughput is

achieved. Jobs are run automatically, and job-management utilities are included. In addition to using AIMS images, the system can also be used with aerial image based inline inspection systems.

2.4 How the Challenges for Mask Defect Disposition based on Aerial Image are Solved

In the following, the same example shown in section 2.3 is used to show how the problems and challenges to Aerial Image Disposition of mask defects are solved.

First, the defect and reference aerial images are aligned by using image alignment algorithms (Figure 6).

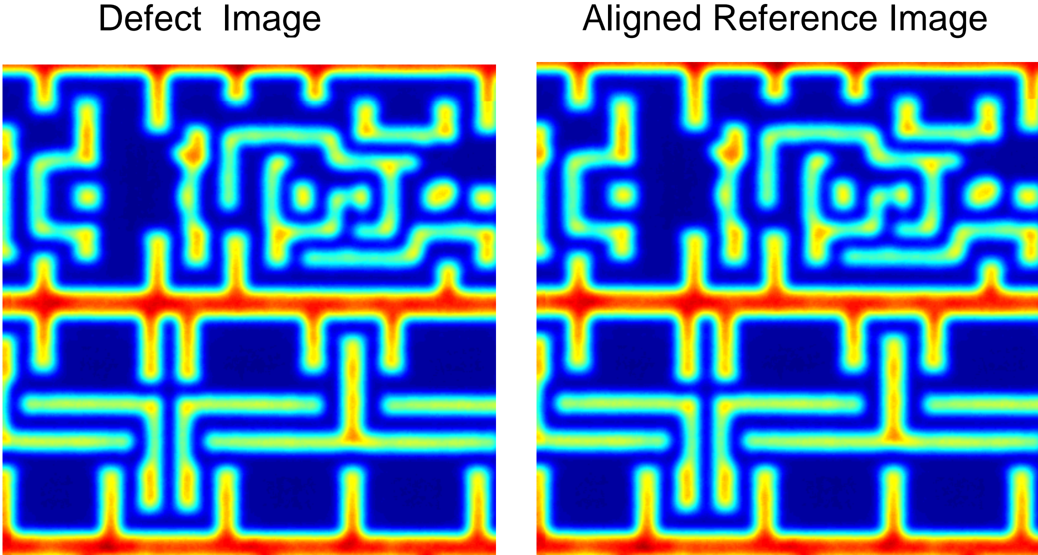

Fig. 6. Solution: 1. Align the defect and reference aerial images

Second, in order to align the defect aerial image with the design GDS, an aerial image simulation on the GDS using an AIMS optical model is performed, and then the real reference aerial image and the simulated aerial image are aligned (Figure 7). This solves the challenge of aligning two different types of images.

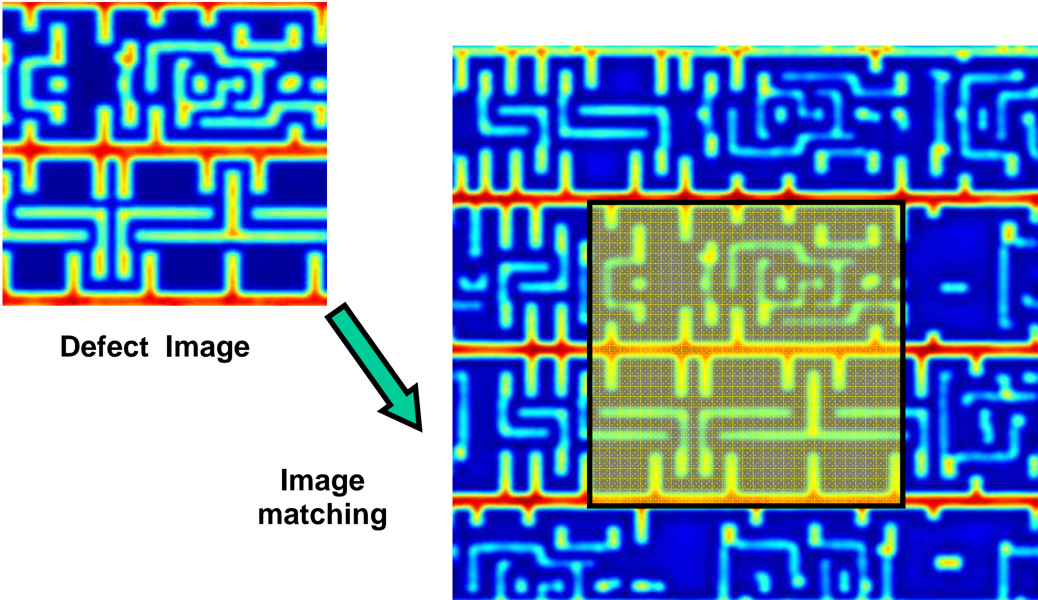

Fig. 7. Solution: 2. Image matching to find the corresponding design

In step 3, once the reference aerial image and design GDS are aligned, the corresponding design clip is cut out, and will be used later to obtain target wafer CD for the defect locations (Figure 8). During this process, the coordinates of the design clips is also converted into the mask coordinates.

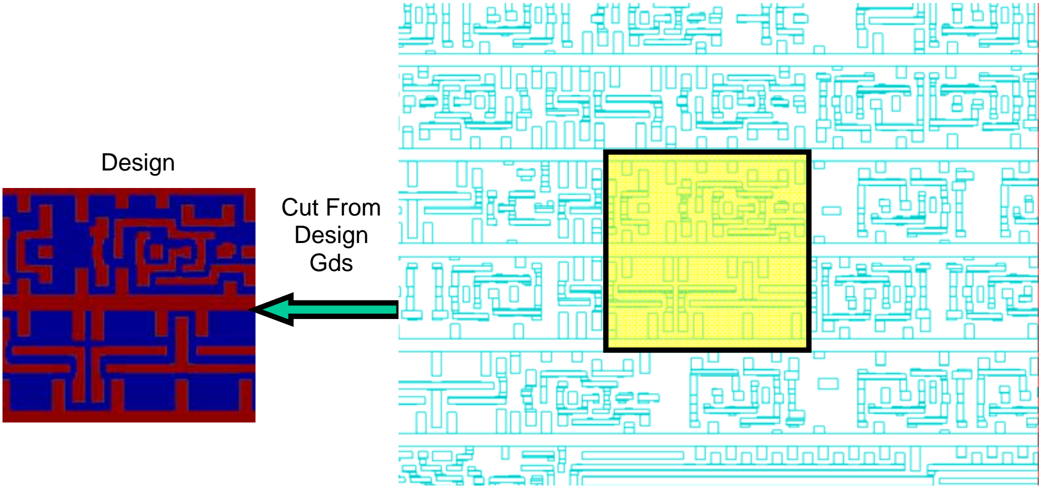

Fig. 8 Solution: 3. Cut the Corresponding Design Clip, and convert GDS coordinate to mask coordinate

Now all of the data required to calculate the wafer CD changes due to defect is available, so that the calculation can be automated. However, performing defect disposition based on a single CD change spec is not accurate enough, and in some cases, incorrect, because (for example) some defects are located at corners while others are on poly layer near the gates, and they should not be treated with the same CD change spec.

Figure 9 shows an example of OPC dissections on typical patterns. In the auto disposition system deployed at TSMC, the patterns are automatically classified into different topologies, such as smooth region, corners, end-to-end, and end-to-smooth regions. Different CD tolerances for defects falling into those different regions are then applied. In addition, the system can also read the cutline location and CD tolerance from the OPC and OPC verification database. This enables different sensitivity levels for different patterns and structures, for example, as also shown in Figure 9, contact coverage regions have higher sensitivity than other region on metal, while metal lines have higher sensitivity than dummy contacts.

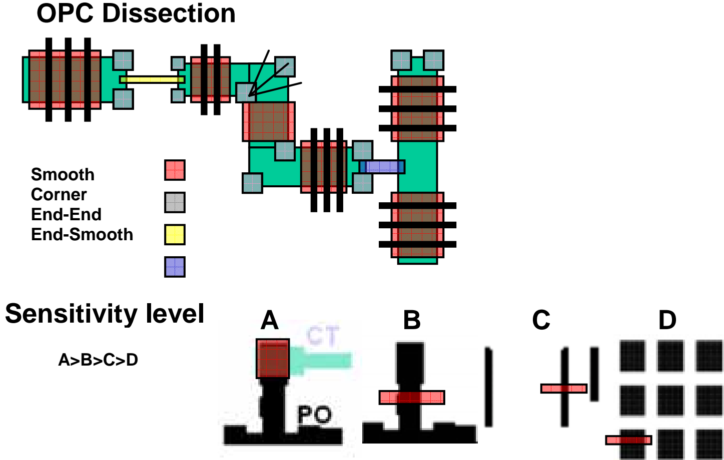

Fig. 9 Solution: 4. Use consistent lithography based specs as OPC and OPC verification

In Luminescent's system, the user can also specify single or multiple cutlines around defects, and all CD changes on those cutline locations are automatically calculated and reported (Figure 10).

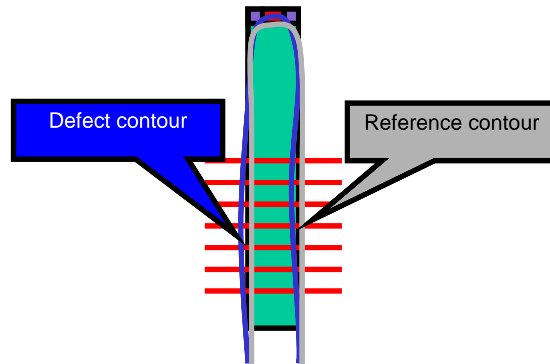

Fig. 10 Solution: 5. Generate multiple cutlines for defect measurements

The LAIPH system provides an intuitive Graphical User Interface (GUI) in both native Linux and Web Browser, enabling operators and engineers to review the final results. As shown in Figure 11, left panel, the GUI shows the defect list, including the disposition decision, defect coordinates, CD changes, etc. On the right panel, the user can see defect and reference AIMS images, the difference between them, the defect map, the aerial image intensity along a selected cutline location, and a zoomed image with design GDS and simulation contours. On the right bottom of the page, the user can write comments, change the disposition decision, and/or go to the next/previous defect. In general the operator is not required to make a decision; however, they do have the power to override the automated disposition decision (i.e., Pass, Waive, and Fail) within the GUI, and may also add additional cutlines for further simulations and calculations.

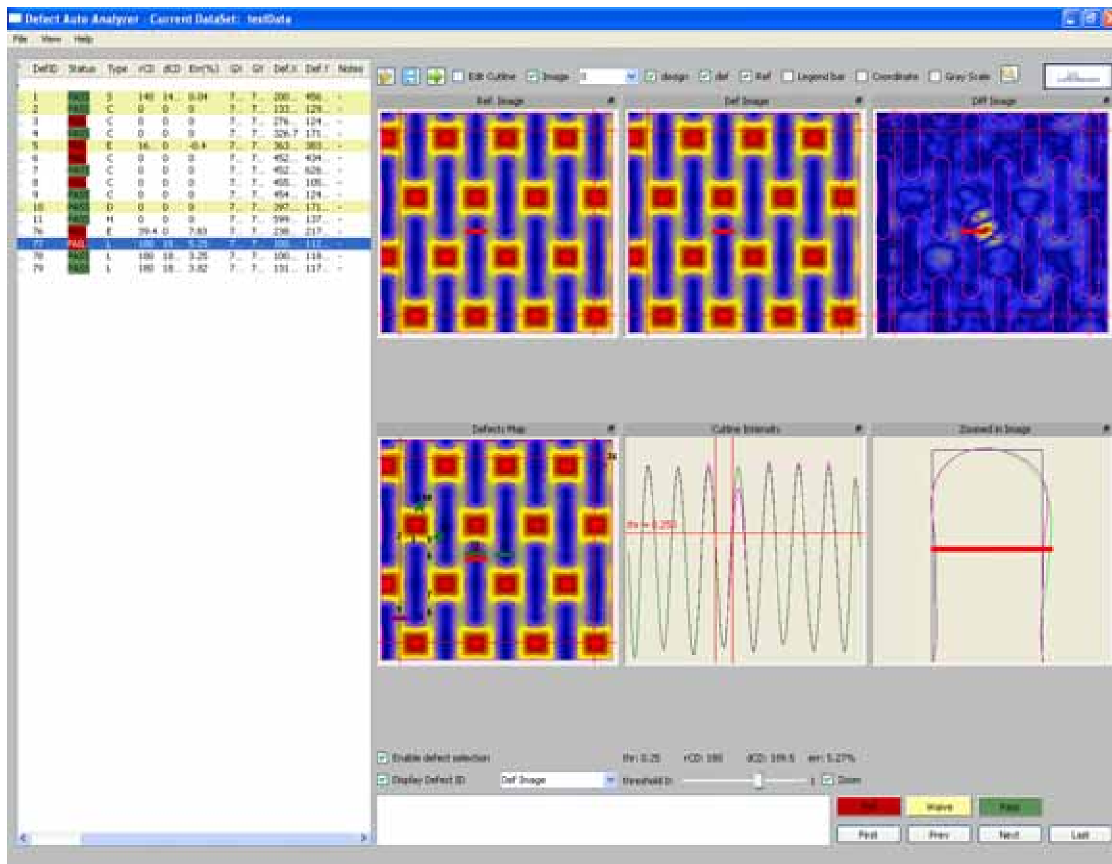

Fig. 11 Solution: 6. The GUI of the aerial image auto disposition system

3. PRODUCTION FLOW AND PRODUCTION RESULTS

3.1 Mask Defect Auto Disposition based on Aerial Image Production Flow

Figure 12 illustrates the production flow of this aerial image based mask defect disposition system as deployed at TSMC. TSMC has mask shops located at three sites – one in Hsinchu, and two in Tainan. At each site, the mask defect coordinates are sent from KLA-Tencor inspection server to AIMS. AIMS takes aerial images from both defect and reference die, and all aerial images from each AIMS are sent to the Luminescent LAIPH system. At the same time, the mask defect coordinates are also sent to the TSMC GDS server to obtain the corresponding GDS clips. Those clips are sent to LAIPH system as well. Once the LAIPH system receives all of the data, it automatically starts the aerial image analysis runs in a distributed mode. The operator and engineers can review the results through the LAIPH Web and native GUI, and adjust the disposition decision when necessary. The final disposition reports are sent to the repair system to repair mask defects.

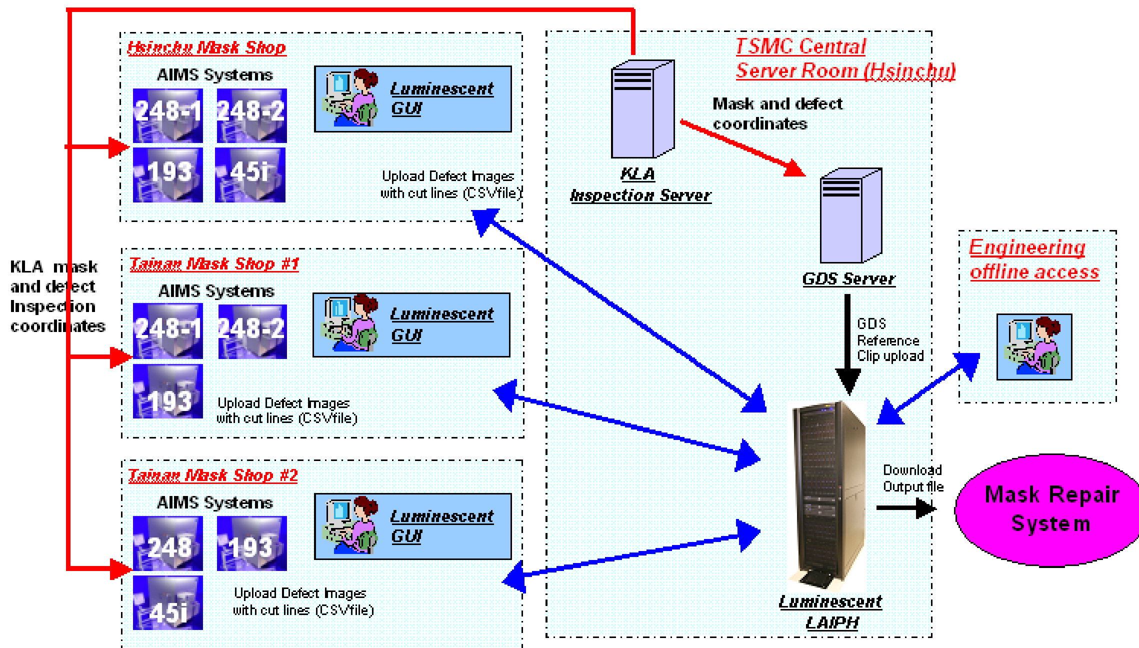

Fig. 12. The TSMC's production flow of mask defect auto disposition based on aerial image

3.2 LAIPH Production Pilot Run Results

Figures 13 to 15 show the pilot run results of LAIPH at TSMC. In Figure 13, the manual measurements performed by operator and auto measurements performed by LAIPH are compared for both a contact mask and a Line/Space (L/S) type of mask. A line of matching slope 1.0 is drawn in each plot of Figure 11, which represents the perfect matching between the manual and auto measurements. The matching on contact and L/S is 0.98 and R^2 is 0.99, indicating excellent matching.

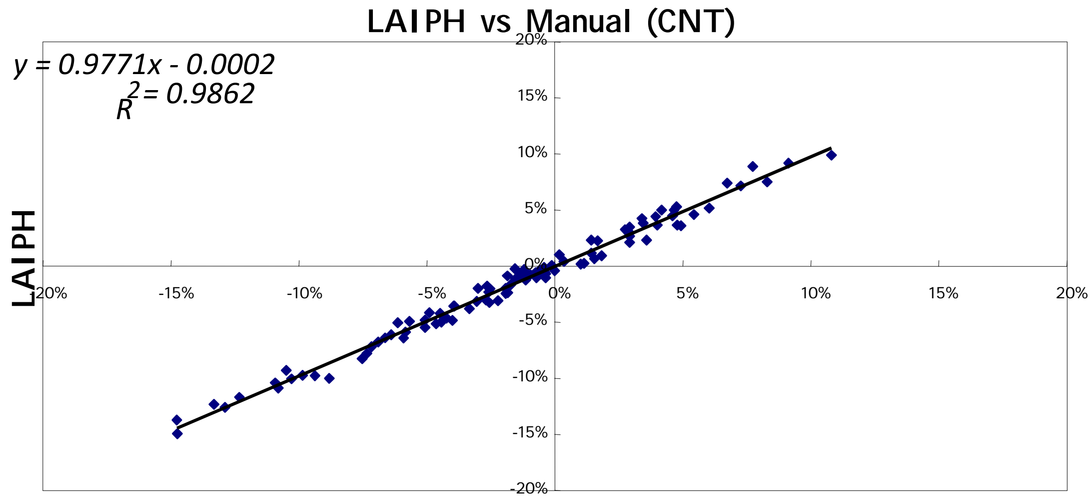

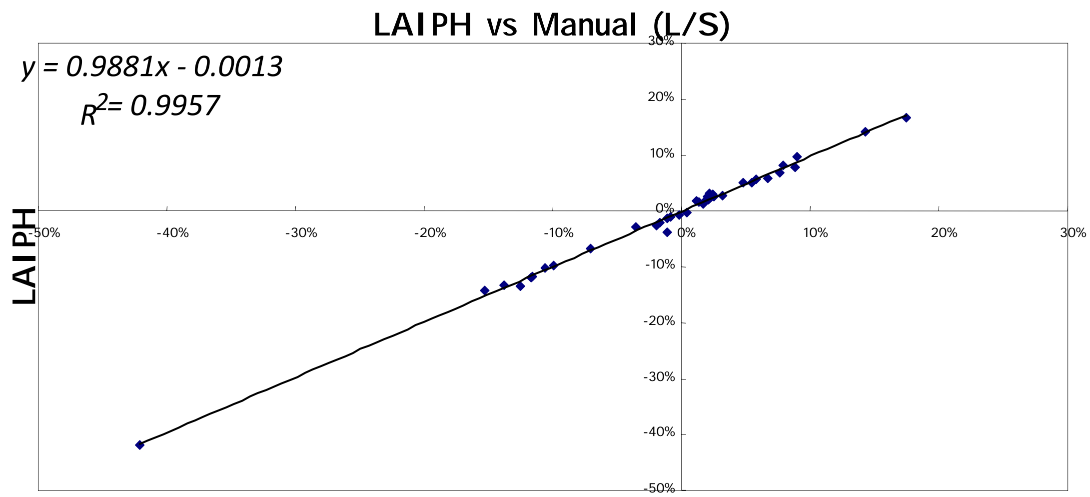

Figure 13. LAIPH production pilot run results - the comparison of LAIPH auto measurements and manual measurements for both L/S and contact layers

After reviewing the data points where the matching was not perfect, it was found that errors were mainly resulted from inadequate manual measurements. For example, as shown in Figure 14, the major error on the contact layer was caused by not being able to detect shift error in the manual operation, so the cutline was always drawn on the center of the defective contact. For the L/S pattern the errors occurred mainly on 2D patterns, where it is difficult for operators to draw the cutline exactly on the center of a rounded feature.

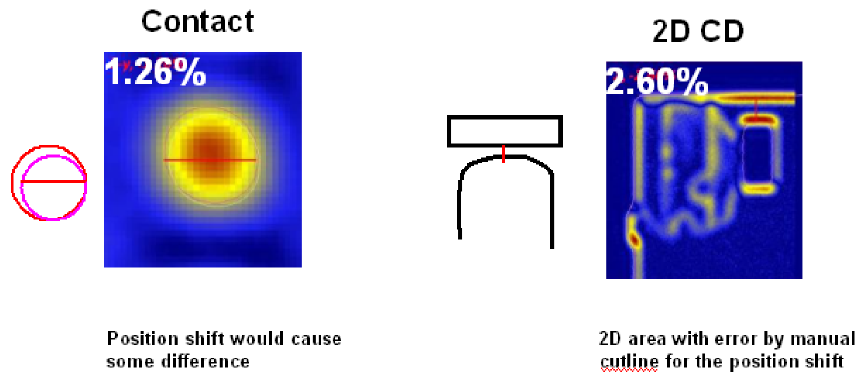

Figure 14. LAIPH production pilot run results that highlights the problems of manual measurements – missing contact shifting issue and difficult to draw the cutline at the right location on rounded feature.

Throughput improvement using LAIPH auto measurements is significant. As shown in Figure 15, it took an operator 40 minutes to perform the X/Y measurements on 17 blind or mis-sized defects, while it only took LAIPH 1 minute to have the entire mask checked and measured the X/Y size. In addition, LAIPH automation also detects the contact shift issue that manual operation cannot detect.

Manual mode :

- Only check abnormal CD in X/Y
- Cycle time 40min

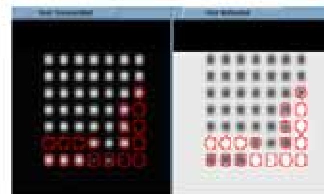

Auto mode:

- Check full field CD and space in X/Y
- Cycle time 1min

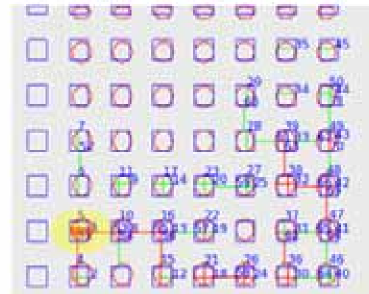

Figure 15. LAIPH production pilot run results – comparing the throughput between manual measurements and auto measurements using LAIPH.

4. SUMMARY AND CONCLUSIONS

Mask defect auto disposition based on aerial image is required for advanced technology nodes, such as 45nm and beyond. The first step to apply such an auto disposition system is on AIMS. The current common practice, semi-manual measurement based on single threshold or peak intensity on an AIMS image, is no longer sufficient, because it is time consuming and inconsistent with the litho spec used in OPC, and during OPC verification.

The automation solution deployed at TSMC mask shop eliminates operator error, significantly improves the throughput, and uses the consistent spec as OPC verification. The production pilot run data demonstrates this system can be deployed into a mask production environment as a standard procedure for mask inspection and defect disposition.

REFERENCES

[1] Abrams, S. and Pang, L., “Fast inverse lithography technology”, 31st Internal Symposium of Microlithography, Proc. SPIE 6154 (2006).

[2] Pang, L., et al, "Inverse Lithography Technology (ILT), What is the Impact to Photomask Industry?", Proc. SPIE 6283, (2006)

[3] Pang, L., et al, "Inverse Lithography Technology (ILT): Keep the balance between SRAF and MRC at 45and 32 -nm", Proc. SPIE 6730, (2007)

[4] Pang, L., et al, " Validation of Inverse Lithography Technology (ILT) and Its Adaptive SRAF at Advanced Technology Nodes ", Proc. SPIE 6924, (2008)

[5] Prins, S. L., et al, "Inverse Lithography as a DFM Tool: Accelerating Design Rule Development with Model-Based Assist Feature Placement, Fast Optical Proximity Correction and Lithographic Hotspot Detection", Proc. SPIE 6924, (2008)

[6] Xiao, G., et al, " Source Optimization and Mask Design to Minimize MEEF in Low K1 Lithography", Proc. SPIE 7028, (2008)

[7] Maurer, W., “Mask specifications for 193 nm lithography,” 16th Annual BACUS Symposium on Photomask Technology and Management, Proc. SPIE 2884, 562-571 (1996)